Photochemistry and Photobiology Vol. 43, No. 1, pp. 71 – 79, 1986
Printed in Great Britain.

0031-8655/86 $03.00+0.00

ANALYSIS OF FLUORESCENCE KINETICS AND ENERGY TRANSFER IN ISOLATED α SUBUNITS OF PHYCOERYTHRIN FROM *Nostoc* sp.

A. J. DAGEN[1], R. R. ALFANO[1]*, B. A. ZILINSKAS[3] and C. E. SWENBERG[2]

[1]Institute for Ultrafast Spectroscopy and Lasers, Department of Physics, The City College of the City University of New York, NY 10031, [2]Radiation Sciences Department, Armed Forces Radiobiology Research Institute, Bethesda, MD 20814, and [3]Department of Biochemistry and Microbiology, Cook College, Rutgers University, New Brunswick, NJ 08903, USA

(*Received* 21 *February* 1985; *accepted* 31 *July* 1985)

Abstract—The fluorescence decay profiles, relative quantum yield, and transmission of the phycoerythrin α subunit, isolated from the photosynthetic antenna system of *Nostoc* sp., were measured using single picosecond laser excitation. The fluorescence decay profiles were found to be intensity independent for the intensity range investigated (4×10^{13} and 4×10^{15} photons-cm^{-2} per pulse). The decay profiles were fitted to a model assuming both chromophores absorb and fluoresce. The inferred total deactivation rates for the two chromophores, in the absence of energy transfer and when the effects of the response time of the streak camera and the finite pulse width are properly included, are 1.0×10^{10} s^{-1} and 1.0×10^{9} s^{-1} for the s and f chromophores, respectively, whereas the transfer rate between the two fluorophores is estimated to be 1.0×10^{10} s^{-1} giving a s → f transfer rate on the order of (100 ps)$^{-1}$. Steady-state polarization measurements were found to be equal to those calculated using the rate parameters inferred from the kinetic model fit to the fluorescence decays. The apparent decrease in the relative fluorescence quantum yield and increase of the relative transmission with increasing excitation intensity is suggestive of ground state depletion and upper excited state absorption. Evidence suggests that exciton annihilation is absent within isolated α subunits for the intensity range investigated (4×10^{13} to 4×10^{15} photons-cm^{-2} per pulse).

INTRODUCTION

Photosynthetic organisms have evolved a number of light harvesting antenna systems for the primary purpose of absorbing sunlight and transferring the absorbed energy to reaction centers. In red and blue-green algae, the light-harvesting system consists of an aggregation of phycobiliproteins, namely phycoerythrin, phycocyanin, and allophycocyanin, which collectively form the phycobilisomes. Each phycobiliprotein is composed of two dissimilar polypeptide chains, the α and β subunits, to which chromophores are covalently bonded. The number and the chemical nature of the chromophores depend on the origin and spectroscopic class of the phycobiliproteins. For *Nostoc* sp. the α and β subunits of phycoerythrin have two and four chromophores respectively. The α and β subunits assemble into aggregates and the trimer form $[(\alpha\beta)_3]$ has dimensions of approximately a right circular disk of radius 60 Å and height 30 Å (Bryant *et al.*, 1979).

Fluorescence measurements on intact phycobilisomes have demonstrated that the route of energy migration within phycobilisomes occurs from phycoerythrin *via* phycocyanin to allophycocyanin (Porter *et al.*, 1978; Grabowski and Gantt, 1978a,b). The concept of energy transfer within the subunits is 14 years old. It was first introduced in the landmark papers of Teale and Dale (Teale and Dale, 1970; Dale and Teale, 1970). Using steady state fluorescence spectra and polarization data, they developed the concept of 's' (sensitizing) chromophores transferring energy to 'f' (fluorescing) chromophores within the subunits. Zickendraht-Wendelstadt *et al.* (1980) used steady state measurements to show that both the 's' and 'f' chromophores of the α and β subunits and the monomer of *Pseudanabaena* W1173 fluoresce. Holzwarth *et al.* (1983) and Hefferle *et al.* (1984) demonstrated that the short life-time components of the fluorescence are related to energy transfer.

The investigation of this energy transfer by examining the picosecond kinetics in isolated phycobiliproteins have led to apparently contradictory results. Kobayashi *et al.* (1978) attributed the short-lived component of the biexponential decay in absorption kinetics in different aggregation states of C-Phycocyanin to the intraprotein energy transfer. They reported s → f transfer times of 32–85 ps. In these higher aggregate forms $[(\alpha\beta)_3$ and larger], however, fluorescence and absorption kinetic measurements as a function of pulse intensity by Doukas *et al.* (1981) indicated that the short decay component was caused by singlet–singlet annihilation effects. If 's' to 'f' transfer was occurring, its effects were masked by the bimolecular interactions. They contended that if s → f transfer existed it occurred in less than 12 ps. These two apparently contradictory interpretations of similar picosecond

*To whom correspondence should be addressed.

kinetic data has left the question of whether intraprotein energy transfer or other phenomena are being detected by these techniques. The purpose of this paper is to clarify this question by providing the first kinetic experimental evidence of s → f transfer by fitting an appropriate model to the fluorescence kinetic data from the α subunit.

In this paper, the intramolecular energy transfer and fluorescence properties of the α subunit of phycoerythrin isolated from *Nostoc* sp. are characterized, using picosecond laser spectroscopy. In contrast to experiments on intact phycobilisomes and isolated phycobiliproteins where it is well known that singlet–singlet annihilation occurs at high excitation intensities (Wong *et al.*, 1981), the experiments reported herein indicate the absence of exciton fusion within the α subunit for the intensity range investigated (4×10^{13} to 4×10^{15} photons-cm^{-2} per pulse). This permits us to describe the kinetics by models assuming 's' to 'f' transfer. Our analysis represents the first attempt to computer simulate the energy transfer dynamics in the α subunit. We describe the α subunit as consisting of two fluorescing chromophores, with the 's' chromophore transferring energy to the 'f' chromophore. The 's' and 'f' chromophores are different spectroscopic forms of the same phycoerythrobilin chromophore. It is concluded that the 's' and 'f' chromophores fluoresce with lifetimes in the absence of energy transfer of 100 ps and 1 ns, respectively. The s → f transfer rate is estimated to be $(100 \text{ ps})^{-1}$.

MATERIALS AND METHODS

Nostoc sp. (strain Mac) was grown in a 14 liter fermentor with pink or cool white fluorescent light as described by Zilinskas and Howell (1983). Phycobilisomes were isolated from these cells according to the protocol of Troxler *et al.* (1980). Phycoerythrin was obtained from dissociated phycobilisomes by use of calcium phosphate chromatography and sedimentation on linear gradients, as detailed by Zilinskas and Howell (1983). The smallest phycoerythrin aggregate so obtained [trimer, $(\alpha\beta)_3$] was removed from the gradient, dialyzed exhaustively against 1 m*M* potassium phosphate, pH 5.0, containing 0.02% sodium azide, and was then lyophilized. This sample was dissolved at ~ 10 mg/mℓ in 8.0 *M* urea, 0.01 *M* potassium phosphate, pH 8.0 and 0.01 *M* β-mercaptoethanol and incubated at 37°C for 2 h. The denatured phycoerythrin was then applied to a DEAE-Sephacel column precquilibrated with the denaturation solution. The α and β subunits were eluted (in that order) with a linear gradient of increasing NaCl in equilibration solution. The peak fractions were pooled separately, dialyzed against 0.1 *M* potassium phosphate, pH 5.0, to effect renaturation, and their identities assessed by absorption, sedimentation on linear gradients, and electrophoresis on SDS-polyacrylamide gels (see Zilinskas and Howell, 1983, for details).

The experimental arrangement used in the fluorescence kinetic measurements is shown in Fig. 1 (Lu *et al.*, 1982). The output of the Nd:glass laser consists of a train of 100 pulses. Pulses in the beginning portion of the train are approximately 10 ps in duration and are spaced ≈ 7 ns apart. A single pulse is selected from the train by applying a 5 ns, 8 kV pulse from a laser triggered spark gap to a Pockels cell situated between crossed polarizers. The selected 1.06 μm pulse is frequency doubled to 8 ps, 0.53 μm pulse by passing the beam through a phase matched potassium di-hydrogen phosphate crystal. The excitation beam is collimated to an elliptical spot size of 2 × 1 mm of uniform intensity at the sample position. The spot size is determined by photographing the image at the sample site using appropriate neutral density filters in front of the film until the excitation pulse is just visible on the film. In addition to determining the spot size, this technique insures the absence of hot spots in the laser pulse. The sample is frontally excited and its fluorescence collected with f 1.25 optics, passed through a Corning 3-67 filter, and focused onto the entrance slit of the streak camera. The output from the phosphor screen of the streak camera is imaged onto an optical multichannel analyzer (OMA) video detector. The digitized trace is stored and processed on a Dec lab PDP 11/03 minicomputer. After normalization both in time and intensity for

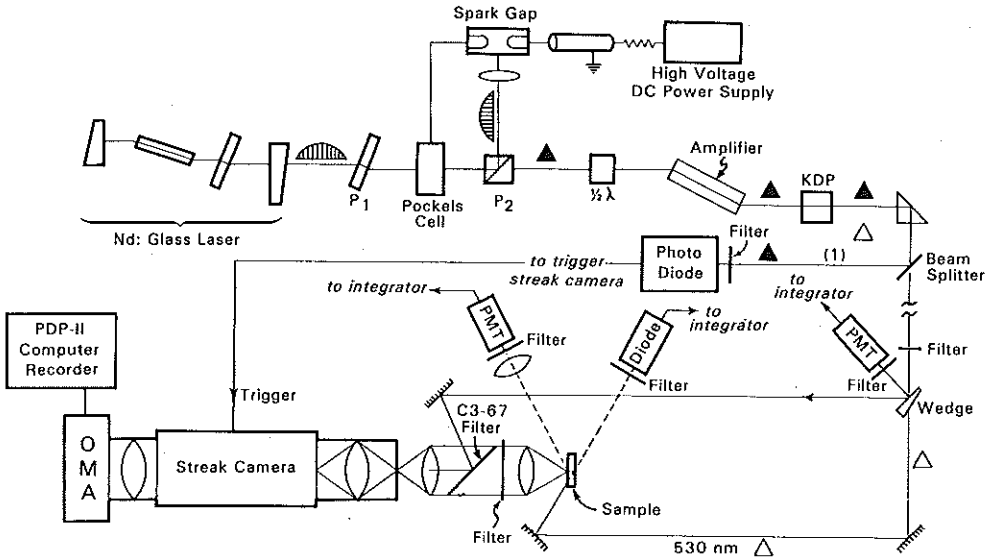

Figure 1. Schematic of experimental apparatus.

nonlinearities in the streak rate, the data were analyzed.

A fraction of the frequency doubled laser pulse is diverted along a separate path to the streak camera. This calibration pulse is well described by a Gaussian $R(t) = I_0 \exp(-t^2/\tau^2)$ with $\tau = 25$ ps on the 2.5 ns time scale and is used to determine the time resolution of the system for that sweep rate. On the 2.5 ns scale, the OMA displays the 8 ps laser pulse with an 8 channel width (FWHM). Because the full scale contains 500 channels each channel on this scale represents 5 ps. The excitation pulse is thus well described by a Gaussian with $\tau = 25$ ps as shown in Fig. 5C. The 2.5 ns scale is used to measure the fluorescence decay kinetics. The 500 ps full scale sweep rate is used to measure the risetimes. The time resolution of the laser-streak camera system on this faster scale is less than 12 ps. The intensity of the excitation at the sample site was determined by a PMT connected to an electronic integrator. A diode located behind the sample and a PMT above the streak camera, both connected to an integrator, measured the intensities of the transmitted and fluorescent beams respectively. The digitized results permitted many shots in a particular intensity range to be examined, thereby resulting in accurate quantum yield measurements. The intensity of the incident fluence was varied by placing appropriate neutral density filters in the excitation pathway. Experiments were performed on the α subunit suspended in 0.1 *M* potassium phosphate at pH 5. The sample OD at the excitation frequency was 0.48. All measurements were made at room temperature.

Absorption spectra were measured on a Cary 17D spectrophotometer. Fluorescence emission spectra were determined on a SLM 4800s spectrofluorimeter with corrections made for the grating and photomultiplier tube efficiency. Samples were diluted to an absorbance of 0.1 at the absorption maximum with 0.1 *M* potassium phosphate, pH 5.0, and were excited at 530 nm. The excitation and emission monochromator bandwidths were 8 and 2 nm, respectively. Fluorescence polarization spectra were measured with an Aminco-Bowman spectrofluorimeter equipped with a R446S (Hamamatsu Corp.) photomultiplier tube and two Glan-Thompson prism polarizers. Measurements and calculation of the degree of polarization were done as described by Grabowski and Gantt (1978a). The excitation and emission monochromator bandpasses were 2.7 and 5.5 nm, respectively; the observation wavelength was at 585 nm. Samples were diluted to an absorbance of 0.17 at the absorption maximum with 0.1 *M* potassium phosphate buffer, pH 5.0.

RESULTS

Figure 2 shows the fluorescence and absorption spectra of the α subunit. The absorption spectrum exhibits a strong peak at ~ 565 nm and a weaker band near 545 nm indicating absorption by 'f' and 's' chromophores, respectively. The measured extinction coefficient at 565 nm is 145 000 M^{-1} cm^{-1}. It is evident from Fig. 2A that the fluorescence is Stokes shifted about 10 nm with its peak occurring at ≈ 575 nm. Assuming mirror symmetry between absorption and emission spectra for the 'f' chromophore allows the total absorption spectrum to be deconvoluted into bands for s and f chromophores. The bands obtained are shown in Fig. 2B; note that for $\lambda > 580$

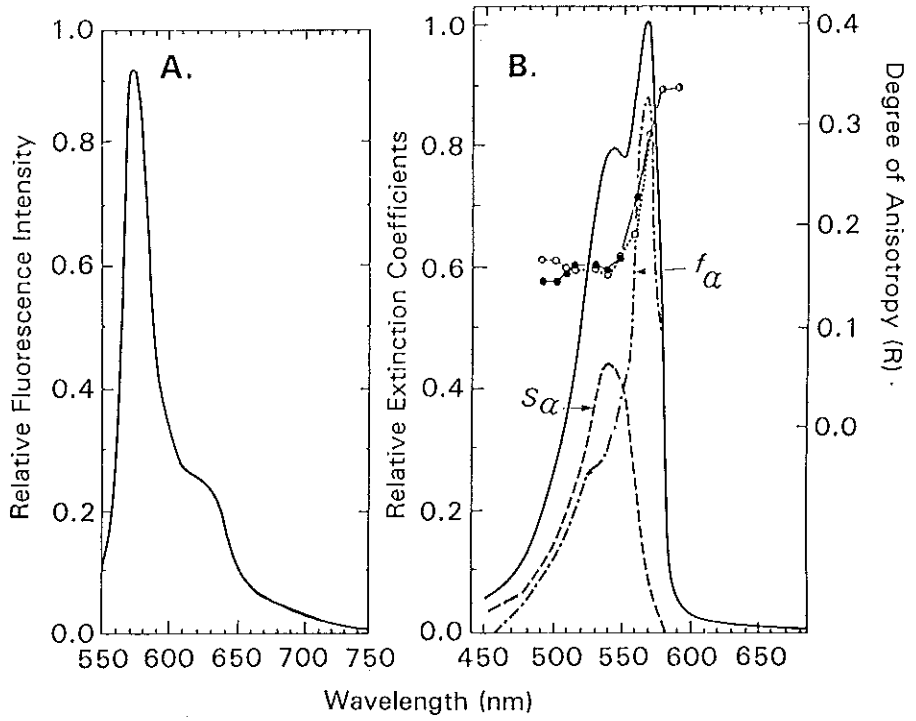

Figure 2. (A) Fluorescence emission spectrum. Excitation wavelength 530 nm. (B) Absorption spectrum of the α subunit and the theoretical deconvolution of the spectrum into its 's' and 'f' components (see text). Theoretical predicted polarization anisotropy *R* (closed circles) derived by fit procedure as described in text (Eq. 9); experimental polarization anisotropy values (open circle). The experimental and theoretical values of *R* for $\lambda > 580$ nm are identical within experimental error.

nm direct excitation of the 's' chromophore is negligible. The deconvolution of the absorption spectrum illustrated in Fig. 2B is very similar to the α-subunit of *Pseudanabaena* W1173 absorption spectrum deconvolution reported by Zickendraht-Wendelstadt *et al.* (1980) and Dale and Teale (1970). The absorption spectrum of the f-chromophore shown in Fig. 2B and that reported by Zickendraht-Wendelstadt *et al.* (1980) both show structure at short wavelengths near the 's'-chromophore absorption peak. At the laser excitation wavelength, 530 nm, the calculated ratio of the f to s absorption coefficients is 0.76.

The fluorescence decay profiles for high and low excitation intensity are illustrated in Fig. 3. The risetime of emission, measured on the 500 ps scale, was within the 12 ps resolution of the streak camera -OMA system on that scale. The shape of the fluorescence profiles was intensity-independent over the intensity range investigated (4×10^{13} to 4×10^{15} photons cm^{-2} per pulse). The shape of the fluorescence kinetics was unchanged when an analyzer was placed at the magic angle of 54.7°. This result is in contrast to the polarization effects noted by other researchers who used cw lasers (Holzwarth *et al.*, 1983; Hefferle *et al.*, 1984). The decay profiles are doubly exponential with an overall e^{-1} time of approximately 1.1 ns. The effect of adding a 2-59 filter in front of the streak camera on the time dependent emission is shown in Fig. 4. The 2-59 filter transmits light of wavelengths beyond 590 nm only. In this case the decay exhibits single exponential behavior with an e^{-1} time of 1.1 ns. The risetimes of emission both in the presence and absence of a filter are within the resolution of the streak camera -OMA system. In contrast to the decay profiles in the absence of the 2-59 filter (Fig. 3), the kinetics display a slight rounding in the emission profiles for $t < 200$ ps when a 2-59 filter is present (Fig. 4). This slight change in shape during the first few hundred picoseconds is evidence for energy transfer from 's' to 'f' fluorophores. This is more evident in Fig. 5, which displays the average of 10 fluorescence decay profiles, without (Fig. 5A) and with (Fig. 5B) the 2-59 filter. Also shown in Fig. 5C is the calibration response curve of the system on the 2.5 ns time scale. It is well described by the expression $R(t) = I_0 \exp(-t^2/\tau^2)$ with $\tau = 25$ ps. The curves in Fig. 6A and B displays the rise portion of the actual experimental data acquired on the fast time scale without and with the presence of a 2-59 filter respectively.

In Fig. 7 is shown the dependence of the relative (apparent) quantum yield and the ratio of transmitted light at high intensity to that at low intensity as a function of single pulse intensity. It is to be noted that the two curves are approximately mirror images of each other with both breaking from unity at an incident fluence of approximately 3 to 4 × 10^{14} photon cm^{-2}.

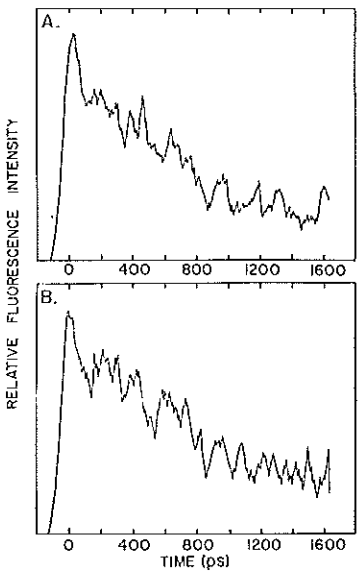

Figure 3. (A) Fluorescence kinetic profile; excitation wavelength 530 nm, 3-67 filter, 200 ps per division. Incident fluence equal to 7.3×10^{13} photons-cm^{-2}. (B) Same as A but for a fluence of 1.43×10^{15} photons-cm^{-2}.

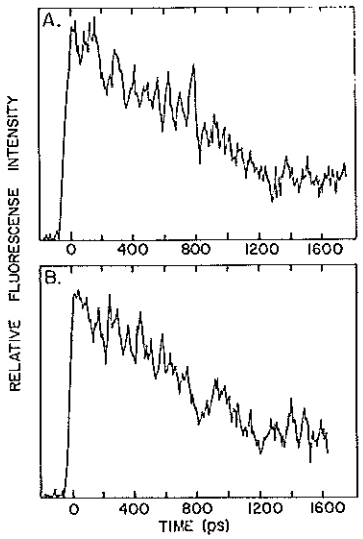

Figure 4. (A) Fluorescence kinetic profile; excitation wavelength 530 nm, 2-59 and 3-67 filters, 200 ps per division. Incident fluence of 1.18×10^{14} photons-cm^{-2}. (B) Same as (A) but for incident fluence of 1.05×10^{15} photons-cm^{-2}.

DISCUSSION

Analysis of time dependence of fluorescence

We analyze the data in terms of the model illustrated in Fig. 8, where the 's' and 'f' chromophores within the α subunit are assumed fixed at a definite distance and orientation. Neglecting coherence effects (i.e. off-diagonal density matrix elements are

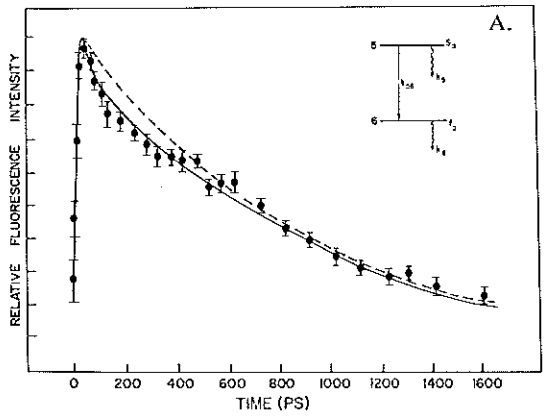

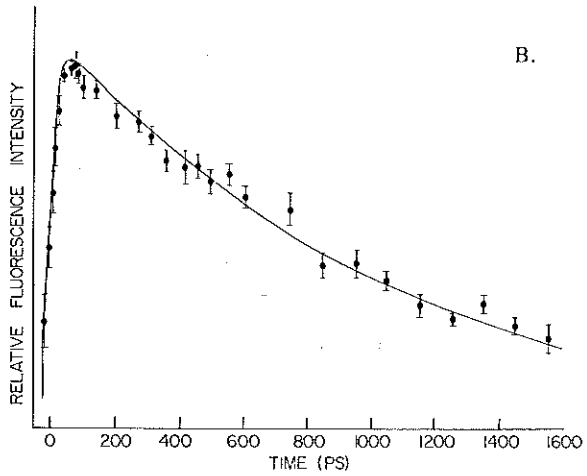

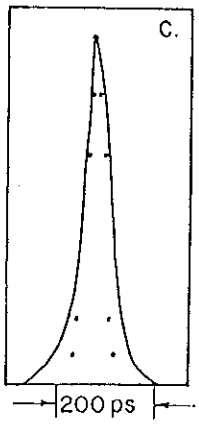

Figure 5. (A) Average of ten fluorescence decays; excitation wavelength 530 nm, incident fluence 7.3×10^{13} photons-cm^{-2} with 3-67 filter. Solid line is best fit to Eq. 3 with $\tau = 25$ ps, $k_s = 1.0 \times 10^{10}\,s^{-1}$, $k_{sf} = 1.0 \times 10^{10}\,s^{-1}$, $k_f = 1.0 \times 10^{9}\,s^{-1}$ and k_{sf}:k_{fr} = 0.8:1.2. Dashed line is fit when k_{sf} is doubled. Error bars are shown for averaged fluorescence curve. (B) Decay profile in presence of 3-67 and 2-59 filter, solid line is fit to Eq. 4 for same rate constants as in (A) with C = 0.1. Error bars are shown for averaged fluorescence curve. (C) Response curve of the system (solid line) and fit to expression $R(t) = I_0 \exp(-t^2/\tau^2)$ for $\tau = 25$ ps (solid dots).

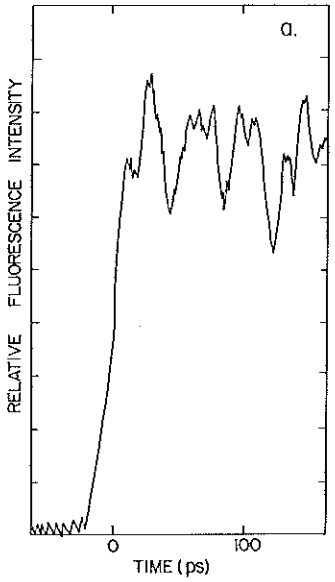

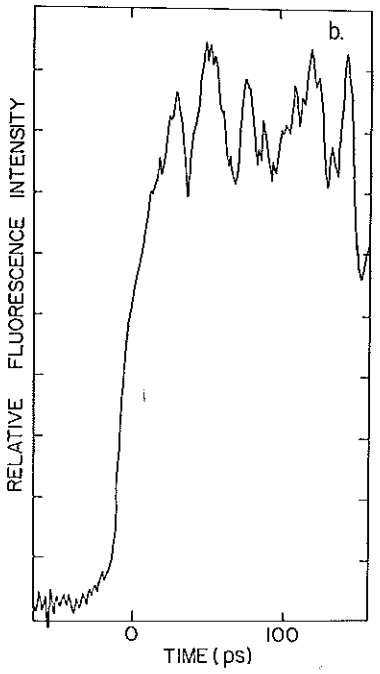

Figure 6. Fluorescence kinetics decays during the first 150 ps on the fast time scale without (a) and with (b) a C.S. 2-59 filter.

set equal to zero) allows the rate equations to be written as

$$\frac{d\rho_s}{dt} = \alpha_s I(t) - (k_s + k_{sf})\,\rho_s(t) \qquad (1)$$

$$\frac{d\rho_f}{dt} = \alpha_f I(t) - k_f\,\rho_f(t) + k_{sf}\,\rho_s(t) \qquad (2)$$

where α_s and α_f are the absorption coefficients of the 's' and 'f' chromophores and $I(t)$ is the normalized excitation pulse shape. The s $\rightarrow$ f transfer rate is

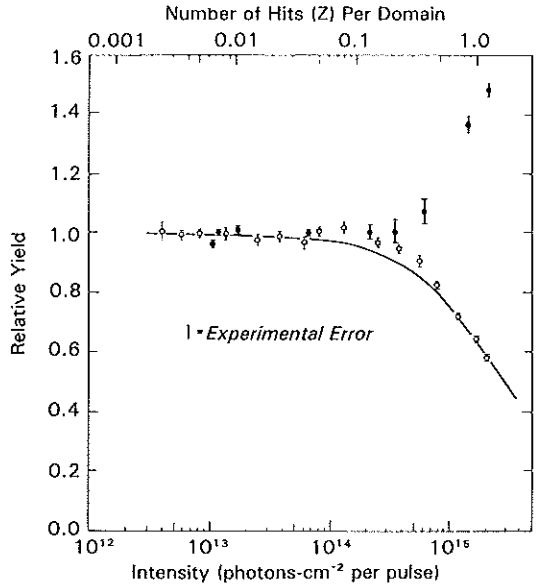

Figure 7. Relative fluorescence quantum yield and transmission as a function of laser single pulse intensity (photons-cm^{-2}); O measured relative quantum yield, ● measured relative transmission. Solid line is fit of apparent relative fluorescence quantum yield to the Paillotin-Swenberg theory with $r = 0.05$.

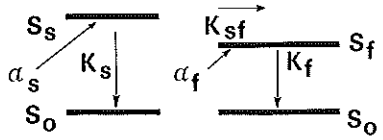

Figure 8. Two component model utilized for the analysis of fluorescence from the subunit. S_0 denotes the electronic ground state and S_s and S_f are the first excited singlet states for the 's' and 'f' moieties, α_s and α_f are the absorption coefficients for these states. k_s and k_f are the total deactivation rates from the s and f chromophores in the absence of energy transfer; k_{sf} is the energy transfer rate from 's' to 'f'.

denoted by k_{sf} and k_s and k_f are the total deactivation rate constants in the absence of energy transfer. Back transfer neglect is justified since the separation in the peaks of the absorption coefficients for 's' and 'f' chromophores imply an energy of activation on the order of 1000 cm^{-1}. A VAX 11/780 computer was used to numerically solve the differential equations describing energy transfer. The equations were solved using a standard Runge–Kutta technique contained in the IMSL library.

The expression for the observed fluorescence when emission from both chromophores is collected simultaneously (in the absence of the C.S. 2-59 filter) is given by

$$F(t) = k_{sr}\,\rho_s(t) + k_{fr}\,\rho_f(t) \qquad (3)$$

where k_{sr} and k_{fr} are the radiation rates of the 's' and 'f' chromophores respectively. When the 2-59 filter is present only wavelengths beyond 590 nm are transmitted and the emission decay profile is given by

$$F(t) = Ck_{sr}\rho_s(t) + (1-C)\,k_{fr}\,\rho_f(t) \qquad (4)$$

C indicates the contribution of the 's' chromophore emission to the fluorescence band 590 nm. Our deconvolution of the absorption spectra shows that C is very small.

The radiative rates of the 's' and 'f' chromophores were obtained from their respective deconvoluted absorption curves (see Fig. 2B), by using the Einstein relationship

$$k_r = 2.88 \times n^2 \times 10^{-9} \int \frac{(2\tilde{\nu}_0 - \tilde{\nu})^{-3}}{\tilde{\nu}}\,\epsilon\,(\tilde{\nu})\,d\tilde{\nu}\ s^{-1} \qquad (5)$$

Here $\tilde{\nu}_0$ is the wavenumber at the mirror symmetry point, $\epsilon\,(\tilde{\nu})$ is the absorption coefficient at wave number $\tilde{\nu}$, and n is the index of refraction. For the α subunit, n is approximately 1.5 (Dale and Teale, 1970). The integral was done numerically with a mesh size of 2 cm^{-1}. A 10 nm Stokes shift was assumed between the peaks of the absorption and fluorescing curves of the 's' chromophore, as is the case of the 'f' chromophore. For the 's' chromophore, $\tilde{\nu}_0 = 1.83 \times 10^4$ cm^{-1}, whereas for the 'f' chromophore, $\tilde{\nu}_0 = 1.75 \times 10^4$ cm^{-1}. With these assumptions the radiative rates for the 's' and 'f' chromophores are calculated to be 2.1×10^8 s^{-1} and 3.1×10^8 s^{-1} respectively. These numbers are estimated to be accurate to within a factor of 2. The ratio (y) of the calculated radiative rates is therefore, $y = k_{fr}/k_{sr} = 1.5$.

The best fit to the decay kinetics (in the absence of the C.S. 2-59 filter) for $y = 1.5$ gives $k_s = 1.0 \times 10^{10}$ s^{-1}, $k_{sf} = 1.0 \times 10^{10}$ s^{-1} and $k_f = 1.0 \times 10^9$ s^{-1}. These values correspond to an s fluorescence decay rate in the absence of energy transfer of (100 ps)$^{-1}$ and an 'f' fluorescence e^{-1} decay rate of (1.0 ns)$^{-1}$. The s → f transfer rate is determined to be (100 ps)$^{-1}$. Changing any rate parameter by a factor of two yields considerably poorer fit to the data. The effects of doubling the least sensitive parameter k_{sf} is shown in Fig. 5A. The theoretical decay curves were fit to an average of 10 experimental fluorescence decays. These rate constants imply that the efficiency of energy transfer is 50%.

These same rate constants were used to fit the fluorescence kinetics in the presence of the C.S. 2-59 filter. Using Eq. 4 a value of C equal to 0.10 was obtained. Again, the fit (illustrated in Fig. 5B) is estimated to have an accuracy to within a factor of 2 for all rate constants. The excellent fit of this entire curve (including rise-times) using the same rate parameters as in Fig. 5A strengthens our contention that the slight change in shape during the first few hundred picoseconds is due to energy transfer. A value of $\tau = 25$ ps provides a good fit to both the response curve (Fig. 5C) and the rise time of the emission.

For Förster dipole–dipole transfer mechanism (1965)

$$k_{sf} = k_s \left(\frac{R_0}{R}\right)^6 = \frac{1}{\tau_s}\left(\frac{R_0}{R}\right)^6 \quad (6)$$

where τ_s is the lifetime of the donor ('s' chromophore) in the absence of transfer and R_0 is the characteristic Förster distance for the process;

$$R_0^6 = \frac{(9000)\ (\ln 10)}{128\ \pi^5\ N\ n^4}\ \phi_s\ K^2\ J \quad (7)$$

N is Avogadro's number per cubic centimeters, ϕ_s is the donor's emission yield in the absence of energy transfer (i.e. $\phi_s = k_{sr}/k_s = (2.1 \times 10^8)(1.0 \times 10^{10}) = 0.02$; see Table 1), n is the refractive index of the medium and J is the spectral overlap integral. We estimate $J = 0.16 \times 10^{-13}$ cm^6 assuming mirror symmetry for the 's' chromophore and a 10 nm Stoke shift between absorption and emission maximum for the donor. The orientation factor, K^2, is not known. In fact, a specific or average value of K^2 cannot be determined from the transfer depolarization factor alone. We therefore adopt the reasonable value of $K^2 = 1$.

With $K^2 = 1.0$, $n = 1.5$ (as approximated by Dale and Teale) and $\phi_s = 0.02$ Eq. 7 gives $R_0 = 20$ Å. This implies that the distance between the 's' and 'f' chromophores is $R = (k_s/k_{sf})^{1/6}\ R_0 = 20$ Å. To compare this with the "size" of the molecule we note that the approximate volume of the $(\alpha\beta)_3$ unit is 3.2×10^5 Å^3 (Bryant *et al.*, 1979). The α subunit molecular weight is 16 600 daltons which is slightly less than the β subunit which has a molecular weight of 19 500 daltons. If we assume the volume occupied by the α component is in the same ratio to the volume occupied by β component as is the ratio of their weights, and that both are spherical molecules (Mörschel *et al.*, 1980) then the radius of the α subunit is approximately 25 Å. This value compares quite favorably with the theoretical R value of 20 Å; presumably the 's' and 'f' moieties can easily be accommodated within the interior of the α molecule.

The absolute fluorescence quantum yield for the α subunit is given by

$$\phi = \frac{k_{sr}}{1+x}\left\{\frac{k_f + k_{sf}\ (1+x)\ y + k_{s\ xy}}{k_f\ (k_s + k_{sf})}\right\} \quad (8)$$

where $x = \alpha_f/\alpha_s = 0.76$ and $y = k_{fr}/k_{sr} = 1.5$. For the parameters that best fit the experimental fluorescence decay curves $\phi = 0.26$. The experimentally obtained value is 0.46 ± 0.06. The discrepancy may be accounted for by the estimation used in calculating k_{sr}, the radiative rate of the 's' chromophore. In particular use of the Einstein relationship to obtain the radiative rate of a chromophore whose fluorescence spectra is unknown (experimentally) is dependent on both the Stokes shift assumed and use of mirror symmetry between absorption and emission spectra. If k_{sr} were 50% larger than that reported the theoretical value for the quantum yield would be within the error bars of the measured value of ϕ. The kinetics fits show that the value ϕ_s (donor's emission yield in the absence of energy transfer) is accurate to within a factor of two. The value of K^2 is also estimated to be within a factor of two. Assuming J is accurate to within a factor of 1.5, R_0 and hence R have an estimated accuracy of approximately 50%. This is quite reasonable for data obtained from kinetic fits. Most of the errors are due to the inherent approximations involved in obtaining the deconvoluted absorption spectra of each chromophore and use of Einstein's relationship to derive the radiative rates.

Degree of polarization anisotropy

A characteristic feature of the measured anisotropy (R) reported in Fig. 2B is the presence of very little structure and nearly constant value of 0.16 for wavelengths between 480 and 550 nm, its monotonic increase for $\lambda \approx 550$–570 nm, and its saturation at 0.34 for $\lambda > 580$ nm. This functional behavior is similar to that reported by Zickendraht-Wendelstadt *et al.* (1980) for the α subunit isolated from *Pseudanabaena* W1173 C-phycoerythrin. Consistency of the experimental values of R ($=R_m$) with the deconvoluted absorption spectrum is afforded by comparing R_m with the calculated weighted sum of the anisotropy (R_w) of the individual absorption band i.e.:

$$R_w = \frac{\alpha_s(\lambda)R_s + \alpha_f(\lambda)R_f}{\alpha_s(\lambda) + \alpha_f(\lambda)} \quad (9)$$

where R_s and R_f are the degree of anisotropy associated with direct excitation of the 's' and 'f' chromophores respectively. Values of R_s and R_f were obtained as follows. For $\lambda > 580$ nm, $\alpha_s(\lambda) = 0$ giving $R_w = R_f = 0.34$, the measured value of R. The value for R_s was inferred from $R_m = 0.16$ at 530 nm where $\alpha_f(\lambda)/\alpha_s(\lambda) = 0.76$. Values of R at other wavelengths were calculated using the deconvoluted spectral data given in Fig. 2B. It is evident that the agreement between R_w and R_m reported in Fig. 2B indirectly

Table 1. Rate constants (units s^{-1}) for the α subunit of *Nostoc* sp. (See Fig. 8); values in parentheses are times in (ps)

$k_s = 1.0 \times 10^{10}$ s^{-1} (100 ps)	$k_f = 1.0 \times 10^9$ s^{-1} (1000 ps)
$k_{sr} = 2.0 \times 10^8$ s^{-1} (5000 ps)	$k_{fr} = 3 \times 10^8$ s^{-1} (3333 ps)
Transfer rate $= k_{sf} = 1.0 \times 10^{10}$ s^{-1} (100 ps)	

supports the deconvolution procedure.

Further support for the kinetics and the measured anisotropy is provided by demanding consistency between calculated anisotropy (as a function of wavelength) utilizing the rate parameters inferred from fluorescence time-dependent measurements and the steady-state anisotropy data. The steady-state anisotropy can be written in terms of the dimer kinetic parameters (Tanaka and Mataga, 1980) as:

$$R = 0.34 + \frac{z\, k_{fr}k_{sf}}{5\{ \times k_{fr}(k_s + k_{sf}) + k_{sr}k_f + k_{fr}k_{sf}\}} \quad (10)$$

where $x = \alpha_f(\lambda)/\alpha_s(\lambda)$ and $z = 3(\cos^2\gamma - 1)$; γ is the angle formed by the emission dipole of the 's' chromophore and the absorption moment of the 'f' chromophore. The constant 0.34 denotes the value of the anisotropy at long wavelength. In adopting this value we have arbitrarily changed the theoretical limiting value of 0.4 to 0.34. This discrepancy arises from the slight differences in the absorption and emission transition moments of either the 's' or 'f' chromophores or both moieties. This point will not concern us here. Values of R, calculated by Eq. 10 using the kinetic parameters given in Table 1 and the deconvoluted absorption spectra, fit the experimental data as well as, if not better than those calculated using Eq. 9. The inferred value of $\gamma = 59°$ is quite similar to the value of 49° determined by Zickendraht-Wendelstadt *et al.* (1980) for *Pseudanabaena* W1173.

Analysis of apparent quantum yield and transmission on intensity

The apparent fluorescence quantum yield dependence on excitation intensity as shown in Fig. 7 has a functional form similar to that predicted by exciton annihilation theories (Swenberg *et al.*, 1976; Paillotin *et al.*, 1979). For the parameter selection of $r = 0.05$, $Z = 0.5$ and $k = 8.76 \times 10^8\ s^{-1}$, the exciton fusion theory of Paillotin *et al.* (1979) fits the relative yield (defined as the integrated fluorescence intensity normalized to low excitation emission intensity) *vs* intensity, as indicated by the solid line in Fig. 7. Without additional experimental data, such as time-dependence fluorescence measurements and transmission data over a broad excitation intensity range, this agreement is suggestive of exciton annihilation processes. The exciton theory of Paillotin *et al.* (1979) does not include the non-linear optical effects produced by ground state depletion or upper excited state absorption and is well known to be applicable only in cases where transmission is unchanged over the intensity domain measured (Breton and Geacintov, 1980) in contrast to the transmission results reported in Fig. 7. Hence, the apparent decrease in the fluorescence yield cannot be attributed solely to singlet exciton fusion. Further evidence against exciton annihilation is the observation that the emission decay, although non-exponential over the excitation intensity domain studied, is independent of laser intensity. When exciton annihilation processes are operative, the fluorescence decay profiles are expected to be non-exponential and excitation intensity dependent. We cannot, at this time, offer a quantitative explanation for the single laser pulse data reported in Fig. 7. The observation that the relative transmission (T_R) and apparent fluorescence yield (ϕ_R) are approximately mirror reflections (about the unit axis) of each other is strongly suggestive of ground state depletion since a three level model, under steady state excitation, gives $\phi_R = T_R^{-1}$ when the excitation intensity is less than the saturation intensity, defined as the incident intensity required to obtain a fluorescence yield decrease of 50% compared to low intensity yield. These remarks suggest that the major contribution to the apparent decrease in ϕ_R and the corresponding increase in T_R is ground state depletion although it does not rule out non-linearities in T_R and ϕ_R due to upper excited state absorption. The absence of exciton annihilation allows the solutions of equations describing energy transfer to explain the decay kinetics by s → f transfer. In larger aggregates of α and β subunits bimolecular processes may mask the observation of the s → f transfer process.

CONCLUSION

The time dependent fluorescence profiles, apparent quantum yield and transmission from the phycoerythrin α subunit isolated from *Nostoc* sp. have been measured over a wide excitation intensity range using a single pulse picosecond source. Kinetics of the fluorescence are quantitatively accounted for using a simple model that assumes both moieties (s and f) absorb and fluoresce. The kinetic parameters characterizing the chromophores have been inferred. This experiment constitutes the first measurement of the s → f transfer in the α subunit. The Förster transfer critical distance (R_0) and the distance between the s and f moieties were calculated. The apparent decrease in the fluorescence yield is attributed to ground state depletion and upper excited absorption. The non-exponential intensity independent fluorescence decays are inconsistent with an exciton annihilation mechanism and are best accounted for in terms of the two component model. Our results strongly suggest that annihilation processes do not occur in isolated α-subunits for fluences less than 4×10^{15} photon-cm^{-2}. The absence of exciton fusion permits the quantitative analysis of the fluorescence kinetics to a model with s → f transfer with both chromophores fluorescing. The s → f rate in the α unit is $(100\ ps)^{-1}$.

Acknowledgements—A. Dagen and R. Alfano thank NSF, PSC-BHE, AFOSR, and NIH for support and B. A. Zilinskas acknowledges support of the State and U.S. Hatch Funds and a USDA competitive grant 5901-0410-8-0185-0.

REFERENCES

Breton, J. and N. E. Geacintov (1980) Picosecond fluorescence kinetics and fast energy transfer processes in photosynthetic membranes. *Biochim. Biophys. Acta* **594**, 1–32.

Bryant, D. A., G. Guglielmi, N. Tandeau deMarsac, A. M. Castets and G. Cohen-Bazie (1979) The structure of cyanobacterial phycobilisomes: a model. *Arch. Microbiol.* **123**, 113–127.

Dale, R. E. and F. W. J. Teale (1970) Number and distribution of chromophore types in native phycobiliproteins. *Photochem. Photobiol.* **12**, 99–117.

Doukas, A. G., V. Stefancic, J. Buchert, R. R. Alfano and B. A. Zilinskas (1981) Exciton annihilation in the isolated phycobiliproteins from the blue-green alga *Nostoc* sp. Using picosecond absorption spectroscopy. *Photochem. Photobiol.* **34**, 505–510.

Förster, Th. W. (1965) Delocalized excitation and excitation transfer, In *Modern Quantum Chemistry* (Edited by O. Sinanoglu), pp. 93–137. Academic Press, New York.

Grabowski, J. and E. Gantt (1978a) Photophysical properties of phycobiliproteins from phycobilisomes: fluorescence lifetimes, quantum yields and polarization spectra. *Photochem. Photobiol.* **28**, 39–45.

Grabowski, J. and E. Gantt (1978b) Excitation energy migration in phycobilisomes: comparison of experimental results and theoretical predictions. *Photochem. Photobiol.* **28**, 47–54.

Hefferle, P., W. John, H. Scheer and S. Schneider (1984) Thermal Denaturation of monomeric and trimeric phycocyanins studies by static and polarized time-resolved fluorescence spectroscopy. *Photochem. Photobiol.* **39**, 221–232.

Holzwarth, A. R., J. Wendler and W. Wehrmeyer (1983) Studies on chromophore coupling in isolated phycobiliproteins 1. picosecond fluorescence kinetics of energy transfer in phycocyanin 645 from *Chroomonas* sp. *Biochim. Biophys. Acta* **724**, 388–395.

Kobayashi, T., E. O. Degenkolb, R. Berson, P. M. Rentzepis, R. MacColl and D. S. Berns (1979) Energy transfer among the chromophores in phycocyanins measured by picosecond kinetics. *Biochemistry* **18**, 5073–5078.

Lu, P. Y., Z. X. Yu, R. R. Alfano and J. I. Gersten (1982) Picosecond studies of energy transfer of donor and acceptor dye molecules in solution. *Phys. Rev.* **A26**, 3610–3617.

Mörschel, E., Klaus-Peter Koller and Werner Wehrmeyer (1980) Biliprotein assembly in the disc-shaped phycobilisomes of *Rhodella violacea* electron microscopical and biochemical analyses of C-phycocyanin and allophycocyanin aggregates. *Arch. Microbiol.* **125**, 43–51.

Paillotin, G., C. E. Swenberg, J. Breton and N. E. Geacintov (1979) Analysis of picosecond laser-induced fluorescence phenomena in photosynthetic membranes utilizing a master equation approach. *Biophys. J.* **25**, 513–534.

Porter, G., C. J. Tredwell, C. F. W. Searle and J. Barber (1978) Picosecond time-resolved energy transfer in *Porphyridium cruentum*. Part 1. In the intact alga. *Biochim. Biophys. Acta* **501**, 232–245.

Swenberg, C. E., N. E. Geacintov and M. Pope (1976) Bimolecular quenching of excitons and fluorescence in the photosynthetic unit. *Biophys. J.* **16**, 1447–1452.

Tanaka, F. and N. Mataga (1979) Theory of time-dependent photo-selection in interacting fixed systems. *Photochem. Photobiol.* **29**, 1091–1097.

Teale, F. W. J. and R. E. Dale (1970) Isolation and spectral characterization of phycobiliproteins. *Biochem. J.* **116**, 161–169.

Troxler, R. R., L. S. Greenwald and B. A. Zilinskas (1980) Allophycocyanin from *Nostoc* sp. phycobilisomes properties and amino acid sequence at the NH_2 terminus of the α and β subunits of allophycocyanins I, II, and III. *Biol. Chem.* **255**, 9380–9387.

Wong, D. F., F. Pellegrino, R. R. Alfano and B. S. Zilinskas (1981) Fluorescence relaxation kinetics and quantum yield from the isolated phycobiliproteins of the blue-green alga *Nostoc* sp. measured as a function of single picosecond pulse intensity, *I. Photochem. Photobiol.* **33**, 651–662.

Zickendraht-Wendelstadt, B., J. Friedrich and W. Rüdiger (1980) Spectral characterization of monomeric C-phycoerythrin from *Pseudoanabaena* W1173 and its α and β subunits; energy transfer in isolated subunits and C-phycoerythrin. *Photochem. Photobiol.* **34**, 367–376.

Zilinskas, B. A. and D. A. Howell (1983) Role of the colorless polypeptides in phycobilisome assembly in *Nostoc* sp. *Plant Physiol.* **71**, 379–385